

1-Octanol/Water Partition Coefficients of 1-Alkyl-3-methylimidazolium Chloride⁺

Urszula Domańska,* Ewa Bogel-Łukasik, and Rafał Bogel-Łukasik^[a]

Abstract: The solubilities of 1-alkyl-3-methylimidazolium chloride, $[C_n\text{mim}][\text{Cl}]$, where $n = 4, 8, 10,$ and 12 , in 1-octanol and water have been measured by a dynamic method in the temperature range from 270 to 370 K. The solubility data was used to calculate the 1-octanol/water partition coefficients as a function of temperature and alkyl substituent. The melting point, enthalpies of fusion, and enthalpies of solid–solid phase transitions were determined by differential scanning calorimetry, DSC. The solubility of $[C_n\text{mim}][\text{Cl}]$, where $n = 10$ or 12 in 1-octanol is comparable and higher than that of $[C_4\text{mim}][\text{Cl}]$ in 1-octanol. Liquid 1-*n*-octyl-3-methylimidazolium chloride, $[C_8\text{mim}][\text{Cl}]$, is not

miscible with 1-octanol and water, consequently, the liquid–liquid equilibrium, LLE was measured in this system. The differences between the solubilities in water for $n = 4$ and 12 are shown only in α_1 and γ_1 solid crystalline phases. Additionally, the immiscibility region was observed for the higher concentration of $[C_{10}\text{mim}][\text{Cl}]$ in water. The intermolecular solute–solvent interaction of 1-butyl-3-methylimidazolium chloride with water is higher than for other 1-alkyl-3-methylimidazolium chlorides.

Keywords: green chemistry • ionic liquids • phase diagrams • partition coefficients • phase transitions

The data was correlated by means of the UNIQUAC ASM and two modified NRTL equations utilizing parameters derived from the solid–liquid equilibrium, SLE. The root-mean-square deviations of the solubility temperatures for all calculated data are from 1.8 to 7 K and depend on the particular equation used. In the calculations, the existence of two solid–solid first-order phase transitions in $[C_{12}\text{mim}][\text{Cl}]$ has also been taken into consideration. Experimental partition coefficients ($\log P$) are negative at three temperatures; this is evidence for the possible use of these ionic liquids as green solvents.

Introduction

Recently, ionic liquids (ILs) have often been discussed as promising solvents for green chemistry and clean synthesis. This paper follows discussion on physicochemical properties of the new generation of solvents for catalysis and synthesis, which have been demonstrated as potential successful replacements for conventional media in chemical processes.^[1] They are generally salts based on a substituted imidazolium cation and an inorganic anion, such as halide, $[\text{AlCl}_4]^-$, $[\text{BF}_4]^-$ or $[\text{PF}_6]^-$, and are often liquids at room temperature.^[2] Room-temperature ionic liquids (RTILs) are one of the goal of green chemistry because they create a cleaner and more sustainable chemistry. They are an important topic that has received more and more attention in recent years as environmentally friendly solvents.^[3, 4] ILs represent clean industrial technology with significant cost and environmental benefits because they

can be used in many cyclic processes without losses, in contrast to volatile organic compounds (VOC). Clean technology concerns the reduction of waste from an industrial chemical process to a minimum: it requires the rethinking and redesign of many current chemical processes. The use of ionic liquids as solvents is one of main strategies of clean industrial technology.^[1] A major reason for the interest in ILs is their negligible vapor pressure, which decreases the risk of technological exposure and the loss of solvent to the atmosphere.^[3b, 5] The low-temperature ionic liquids which are used as reaction media in many of the catalytic processes, principally based on chloroaluminate(III) ionic liquids, represent first-generation ionic liquid processes. The second-generation ionic liquid processes based on other, more benign, ionic liquids are currently under investigation and development in a variety of laboratories around the world.^[1a] Most ILs are hygroscopic, which has significant practical implications. Qualitative and quantitative vapor–liquid equilibrium and liquid–liquid phase behavior of water and three ionic liquids: 1-*n*-butyl-3-methylimidazolium hexafluorophosphate, ($[\text{bmim}][\text{PF}_6]$), 1-*n*-octyl-3-methylimidazolium hexafluorophosphate, ($[C_8\text{mim}][\text{PF}_6]$), and 1-*n*-octyl-3-methylimidazolium tetrafluoroborate, $[C_8\text{mim}][\text{BF}_4]$, have been reported.^[6] For instance, scientists from the University of Notre

[a] Prof. Dr. U. Domańska, E. Bogel-Łukasik, R. Bogel-Łukasik
Warsaw University of Technology
Faculty of Chemistry, Physical Chemistry Division
Noakowskiego 3, 00-664 Warsaw (Poland)
E-mail: ula@ch.pw.edu.pl

[⁺] Presented at the 17th IUPAC Conference on Chemical Thermodynamics, Rostock (Germany), 28.07.–02.08.2002

Dame^[6] and from The Queen's University of Belfast^[1a] provide some general guidelines on IL/water miscibility. Their work has shown that halide, ethanoate, nitrate, and trifluoroacetate salts are totally miscible with water, while many other salts are immiscible. Salts can be totally miscible or immiscible depending on the substituents on the cation. The solubility of water in the IL-rich phase for $[C_n\text{mim}][\text{PF}_6]$ and $[C_n\text{mim}][\text{BF}_4]$ is a function of chain length between $n = 4-8$ and $6-10$.^[7a] The complete understanding of the phase behavior of ILs with water is an important issue. The presence of water in the IL phase can dramatically affect the physical properties.^[7b,c] The problem of miscibility of ILs with water as well as many other organic solvents can affect properties, as clearly demonstrated for the viscosity and density,^[7a] surface tension,^[7d] and polarity.^[7e] The synthesis methods of ILs have been reported.^[1b, 8] The synthesis methods of halides ILs is described elsewhere.^[8f,g] The problem of partitioning benzene and its substituents between IL $[\text{bmim}][\text{PF}_6]$ /water and 1-octanol/water with regard to a possible use for the liquid-liquid extraction process was presented earlier.^[8b]

We have already reported the solubility of three simple imidazoles in alcohols.^[9] The solubility was found to be lower in alcohols than in water. We have begun systematic investigations into the thermodynamic properties and phase equilibria of simple imidazole molecules,^[9a,b] benzimidazoles,^[9b,c] and phenylimidazoles^[9d] as well as the new class of their ionic salts. The densities, surface tensions, octanol/water partition coefficients, solid-liquid equilibria (SLE), and liquid-liquid equilibria (LLE) of many binary mixtures are under investigation. The solubilities of 1-dodecyl-3-methyl-

imidazolium chloride $[\text{C}_{12}\text{mim}][\text{Cl}]$ in alcohols have already been published.^[10]

The purpose of this paper is to report the solubilities of 1-alkyl-3-methylimidazolium chloride $[\text{C}_n\text{mim}][\text{Cl}]$, where $n = 4, 8, 10, \text{ and } 12$, in 1-octanol and water and to present the 1-octanol/water partition coefficients as a function of temperature and alkyl substituent.

Results and Discussion

Differential scanning calorimetry (DSC): Table 1 shows the DSC results for the pure component, observed from 200 to 400 K. A search of the literature has indicated that data for $[\text{C}_n\text{mim}][\text{Cl}]$, presented here have not been reported previously without $[\text{C}_{12}\text{mim}][\text{Cl}]$, which was described in our previous work.^[10] From the thermographs of pure solutes it can be noted that three of the investigated salts exhibit different crystalline phases. Unfortunately, it is only possible to describe certain DSC peaks for $[\text{C}_{12}\text{mim}][\text{Cl}]$. The mesomorphic plastic phase, α_1 in the region from 369.8 to 310.15 K, has a very small heat of melting transition equal to $0.604 \text{ kJ mol}^{-1}$. On the other hand, the transition of $[\text{C}_{12}\text{mim}][\text{Cl}]$ plastic phase α_1 into crystalline phase β_1 is accompanied by the unbelievably high heat effect equal to $23.580 \text{ kJ mol}^{-1}$; this is the average of five repeats of the DSC experiment. Between 283 and 200 K, the next three solid-solid phase transitions are observed with phase transitions enthalpies (ΔH_{trII} , ΔH_{trIII} , and ΔH_{trIV}) of $< 5\%$ of the previous one. Our solubility measurements were provided only from the melting point of IL to 273 K, thus only the two first solid-solid phase transitions were observed. The solid-solid phase transition temperatures, T_{trI} and T_{trII} of $[\text{C}_{12}\text{mim}][\text{Cl}]$ were confirmed by solubility measurements in 1-octanol as two inflections on the liquidus curve, but at much higher temperatures. We discussed the different temperatures of the solid-solid phase transitions of $[\text{C}_{12}\text{mim}][\text{Cl}]$ for the pure solute and for the binary mixture in our previous work.^[10] These changes may be explained by the changes of crystalline forms as a consequence of the twist of the alkyl chain and by the different packing effect in the hydrogen-bonded network of the salt. Usually, for the other ionic liquids, this effect occurs over a larger number of carbon atoms in the alkyl chain of the molecule.^[8b] Generally, it was observed that, even for the pure substances (packed under nitrogen), the DSC thermographs were not reproducible with the same heat effects. The results of the DSC measurements presented in Table 1 are the average of many samples for different masses.

The only other related salt for which a crystal structure has been determined was $[\text{C}_{12}\text{mim}][\text{PF}_6]$.^[8b] It was noted that the imidazolium ring is completely planar and the straight chain nature of the alkyl group is disrupted close to the ring where it adopts a bent conformation. The $[\text{C}_{12}\text{mim}]^+$ cation was described as having a spoon-shaped structure. For $[\text{C}_{10}\text{mim}][\text{Cl}]$, a high enthalpy of melting was observed ($30.93 \text{ kJ mol}^{-1}$) and the series of small transformations at $\approx 293 \text{ K}$ (negative energy effect), and two transformations at 255 and 245 K, with the enthalpies 1.247 and $0.278 \text{ kJ mol}^{-1}$

Abstract in Polish: *Stosując metodę dynamiczną badano rozpuszczalność chlorków 1-alkyl-3-metyloimidazolu, $[\text{C}_n\text{mim}][\text{Cl}]$, gdzie $n = 4, 8, 10, 12$ w 1-oktanolu i w wodzie w zakresie temperatur od 270 do 370 K. Wyniki badań rozpuszczalności pozwoliły obliczyć współczynniki podziału 1-oktanol/woda w funkcji temperatury i długości podstawnika alkilowego. Za pomocą kalorymetru skaningowego DSC wyznaczono temperatury topnienia, entalpie topnienia oraz temperatury i entalpie przemian fazowych ciało stałe-ciało stałe. Rozpuszczalność soli $[\text{C}_{10}\text{mim}][\text{Cl}]$ oraz $[\text{C}_{12}\text{mim}][\text{Cl}]$ w 1-oktanolu jest porównywalna i nieco większa od $[\text{C}_n\text{mim}][\text{Cl}]$. Ciekły $[\text{C}_8\text{mim}][\text{Cl}]$ wykazuje ograniczoną mieszalność z 1-oktanołem i z wodą i dla tych układów wyznaczono odpowiednie równowagi ciecz-ciecz. Obszar ograniczonej mieszalności obserwowano również dla większych stężeń $[\text{C}_4\text{mim}][\text{Cl}]$ w wodzie. Oddziaływania międzycząsteczkowe substancja rozpuszczona - woda są znacznie większe dla $[\text{C}_4\text{mim}][\text{Cl}]$ niż dla pozostałych soli. Krzywe rozpuszczalności korelowano równaniami UNIQUAC ASM oraz NRTL1 i NRTL2. Odchylenia standardowe wynosiły od 1.8 do 7 K i zależały od rodzaju równania i układu. W obliczeniach uwzględniono dwie przemiany fazowe ciało stałe - ciało stałe. Wartości współczynników podziału ($\log P$) są ujemne, co wskazuje na możliwość zastosowania badanych "cieczy jonowych" jako rozpuszczalniki "sprzyjające środowisku".*

Table 1. Physical constants of pure $[C_n\text{mim}][\text{Cl}]$, as determined from DSC data.

Salt	T_m [K]	ΔH_m [kJ mol ⁻¹]	$T_{\text{trI}}/T_{\text{trII}}/T_{\text{trIII}}/T_{\text{trIV}}$ [K]	$\Delta H_{\text{trI}}/\Delta H_{\text{trII}}/\Delta H_{\text{trIII}}/\Delta H_{\text{trIV}}$ [kJ mol ⁻¹]
$[C_4\text{mim}][\text{Cl}]$	341.95	14.057	(glass) 197.35 ^[a]	
$[C_8\text{mim}][\text{Cl}]$	285.41	0.233	210.85 ^[b]	
$[C_{10}\text{mim}][\text{Cl}]$	311.17	30.932	255.00/245.00	1.247/0.278
$[C_{12}\text{mim}][\text{Cl}]$	369.78	0.604	310.15/283.21/270.61/235.34	23.580/1.157/1.457/0.158

[a] Δc_p at the glass transition is equal to 49.1 J K⁻¹ mol⁻¹. [b] Δc_p at the glass transition is equal to 94.6 J K⁻¹ mol⁻¹.

for the first and second transition, respectively. For $[C_4\text{mim}][\text{Cl}]$, the small peak at ≈ 315 K together with melting transition was observed for the different scan rates. This small effect may be seen as a characteristic inflection in the liquidus curve in 1-octanol and water. It was shown in Tables 2 and 3 as separate crystalline phases α_1 and β_1 . The effect of cool crystallization was also observed at 251.15 K. The glass transition of $[C_4\text{mim}][\text{Cl}]$ was observed at 197.35 K. DSC measurements of the only liquid salt at room temperature, $[C_8\text{mim}][\text{Cl}]$, exhibits a melting temperature of 285.40 K with the enthalpy of melting equal to 232.85 kJ mol⁻¹ after freezing at 200 K. During the solubility measurements it was impossible to obtain the crystalline phase of $[C_8\text{mim}][\text{Cl}]$ even after few hours cooling at 220 K. The glass transition for $[C_8\text{mim}][\text{Cl}]$ was observed at a lower temperature, namely 210.85 K.

For simple imidazoles, only 2-methyl-1*H*-imidazole has shown a solid–solid phase transition with the enthalpy of the solid–solid transition lower than that of fusion.^[9a] On the other hand, the even-numbered *n*-alkanes C₂₀–C₄₄ undergo solid–solid transitions showing different crystalline forms.^[11] The transitions are related to the rotation of molecular chains about their long axes. The atomic structure of the low-temperature crystalline phase of even-numbered paraffins has also been determined.^[11c,d] More recently, the main structural features of the high-temperature rotator phases have been established as well.^[11b] Our solute with the *n* = 12 substituent in the position 1 of the imidazole ring may cause a high degree of orientational disorder of the molecules of hydrogen-bonded network of the ionic liquid.

X-ray crystal analyses of some ILs have already been published by many authors.^[8b,c,f,g, 12] For the ILs molecules composed of a rigid and polarizable core attached to one or two aliphatic chains often give liquid-crystal mesophases when heated; especially salts that contain alkyl chain lengths of *n* > 12.^[8f] Additionally, the phase diagrams for different ILs of the melting point as a function of alkyl chain length *n*, show that C₁₂ is the limit with regards to the melting transitions from crystalline form or clearing point of liquid crystalline form.^[1a, 13] In particular, when the alkyl chains are long, smectic phases tend to form as a result of microphase separation of the polarizable core and the aliphatic tail portions. One of the first long-chain imidazolium salts, whose crystal structure has been reported, was 1,3-didodecylbenzimidazolium chloride, $[(C_{12})_2\text{Bim}][\text{Cl}]$.^[8g] The chain configuration and the lack of any disorder in the structure appear to be a consequence of interdigitated molecular packing. The crystal structure of ILs is very important and is responsible for the solid–liquid and liquid–liquid phase equilibria in binary mixtures of ILs with different solvents.

Solid–liquid equilibria (SLE): The solubilities of $[C_n\text{mim}][\text{Cl}]$ in 1-octanol and water are shown in Tables 2–4. The Tables include direct experimental results of the SLE, or SLE and LLE temperatures (Table 4), T_1 (α_1 , β_1 , or γ_1 stable crystalline

Table 2. Solid–liquid equilibria for $\{[C_4\text{mim}][\text{Cl}]$, or $[C_{10}\text{mim}][\text{Cl}]$, or $[C_{12}\text{mim}][\text{Cl}] + 1\text{-octanol}\}$.

x_1	T_{γ_1} [K]	x_1	T_{β_1} [K]	x_1	T_{α_1} [K]
$[C_4\text{mim}][\text{Cl}]$					
0.2713			213.16	0.8957	338.99
0.3081			282.51	0.9296	340.33
0.3350			289.44	1.0000	341.94
0.3507			299.64		
0.3857			306.60		
0.4240			311.66		
0.4689			317.72		
0.5266			323.23		
0.6074			327.85		
0.6927			332.82		
0.7667			334.88		
0.8282			336.23		
$[C_{10}\text{mim}][\text{Cl}]$					
0.1916					277.50
0.2525					291.93
0.3072					302.68
0.3832					306.74
0.4259					307.61
0.4715					308.04
0.5459					308.20
0.5920					308.36
0.6676					308.52
0.7160					308.96
0.7861					309.16
0.8555					309.99
0.9146					310.98
0.9667					310.93
1.0000					311.17
$[C_{12}\text{mim}][\text{Cl}]$					
0.1864	272.72	0.4638	298.90	0.7508	318.91
0.1947	274.25	0.4861	300.36	0.7647	320.19
0.2154	277.52	0.5142	304.16	0.8000	323.54
0.2350	280.27	0.5459	307.72	0.8264	329.67
0.2551	282.85	0.5818	310.94	0.8508	331.86
0.2888	287.76	0.5951	312.62	0.9316	355.18
0.3004	289.62	0.6186	314.23	1.0000	369.78
0.3340	292.10	0.6406	315.32		
0.3502	292.98	0.6600	315.95		
0.3666	294.25	0.6773	316.66		
0.3725	294.72	0.6978	316.62		
0.3773	294.70	0.7154	316.72		
0.3949	295.37	0.7308	317.26		
0.4166	296.03				
0.4369	296.46				
0.4392	296.55				
0.4526	296.95				

Table 3. Solid–liquid equilibria on $\{[C_n\text{mim}][\text{Cl}], \text{ or } [C_{12}\text{mim}][\text{Cl}] + \text{water}\}$.

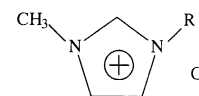
x_1	$T_{\beta 1}$ [K]	x_1	$T_{\alpha 1}$ [K]
[C ₄ mim][Cl]			
0.4291	273.23	0.9446	332.24
0.4702	282.53	0.9736	336.17
0.5145	291.87	1.0000	341.94
0.5440	296.13		
0.5787	302.47		
0.6227	312.03		
0.6314	313.16		
0.6718	316.76		
0.7292	321.01		
0.7675	324.69		
0.8068	326.94		
0.8460	327.64		
0.8891	330.34		
[C ₁₂ mim][Cl]			
0.0964	275.86		
0.1488	288.74		
0.2051	297.36		
0.2514	301.11		
0.3120	303.98		
0.3349	304.27		
0.3675	305.00		
0.3747	304.95		
0.4319		306.73	
0.4713		309.07	
0.4996		310.34	
0.5055		310.78	
0.5260		311.29	
0.5573		313.82	
0.5909		316.12	
0.6517		319.29	
0.6783		321.22	
0.7180		323.64	
0.7816		330.05	
0.8018		333.34	
0.8087		334.61	
0.8440		340.06	
0.8634		343.28	
0.8989		347.85	
0.9437		358.25	
1.0000		369.78	

Table 4. Solid–liquid, SLE and liquid–liquid, LLE equilibria on $\{[C_{10}\text{mim}][\text{Cl}] + \text{water}\}$.

x_1	$T_{\alpha 1}$ [K]	$T_{1\text{LLE}}$ [K]
[C ₁₀ mim][Cl]		
0.2029	273.93	
0.2576	283.43	
0.3228	288.49	
0.3680	292.92	
0.4294	298.42	
0.4855	303.69	307.27
0.5353	306.74	314.13
0.6025	309.56	320.15
0.6275	310.01	322.49
0.6921	310.07	323.73
0.7595	310.60	321.13
0.7996	310.74	318.07
0.8534	310.79	312.38
0.9370	310.98	
1.0000	311.17	

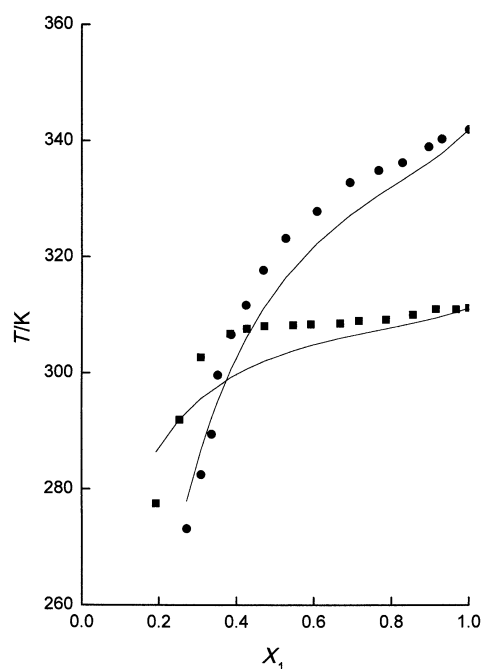
forms) versus x_1 , the mole fraction of the solute, $[C_n\text{mim}][\text{Cl}]$, in the saturated solution for the investigated systems.

The ability of the solute to form hydrogen bonds with potential solvents is an important feature in its behavior. Basically, $[C_n\text{mim}][\text{Cl}]$ ionic liquids can act both as a hydrogen-bond acceptor ($[\text{Cl}]^-$) and donor ($[C_{12}\text{mim}]^+$) and would be expected to interact with solvents which have both accepting and donating sites (Scheme 1).

Scheme 1. Structures of 1-alkyl-3-methylimidazolium chlorides $[C_n\text{mim}][\text{Cl}]$, where $R = C_nH_{2n+1}$ (for $n = 4, 8, 10, \text{ and } 12$).

On the other hand, it is well-known that 1-octanol and water are hydrogen-bonded solvents with both high enthalpies of association and association constants. Hence they would be expected to stabilize solutes with hydrogen-bonded donor sites.

The experimental phase diagrams of SLEs investigated in this work are not easy to interpret because the solutes are a very complicated and highly interacting molecules, especially when the solvent is water or alcohol. The solubility of $[C_n\text{mim}][\text{Cl}]$ in 1-octanol increases in the order $C_{10} < C_{12} < C_4$, which is also indicative for the high concentration of the solute. The results depend on the melting temperature and the enthalpy of melting of the solute. The C_4 salt is more soluble in 1-octanol than C_{10} . For $[C_{12}\text{mim}][\text{Cl}]$, the influence on the solubility and the shape of the liquidus curve has the high value of the enthalpy of solid–solid phase transition. The enthalpy of melting of C_{12} is lowered by the enthalpy of the solid–solid phase transition and this is the main reason for the higher solubility of $[C_{12}\text{mim}][\text{Cl}]$ than $[C_{10}\text{mim}][\text{Cl}]$ (see Figures 1 and 2).

Figure 1. Comparison between the solubility of $[C_4\text{mim}][\text{Cl}]$ and $[C_{10}\text{mim}][\text{Cl}]$, in 1-octanol. Points, experimental results: (●) $[C_4\text{mim}][\text{Cl}]$; (■) $[C_{10}\text{mim}][\text{Cl}]$. Solid lines are calculated by means of the NRTL2 equation.

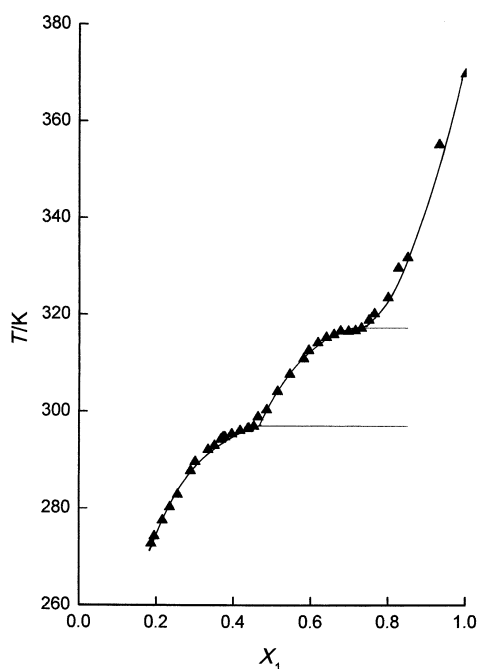


Figure 2. Solubility of $[C_{12}mim][Cl]$ in 1-octanol. Points are the experimental results.

The solubility of $[C_nmim][Cl]$ in water decreases in the order $C_4 > C_{10} > C_{12}$, which means that the short alkane substituent at the imidazole ring results in improved solubility of IL in water. It is mainly evident for the low concentration of solute ($x_1 < 0.6$) (Figures 3–5). The liquidus curve of the 1-*n*-dodecyl-3-methylimidazolium chloride exhibits two characteristic inflections (solid–solid phase transition) in 1-octanol and only one in water (Figures 2 and 5).

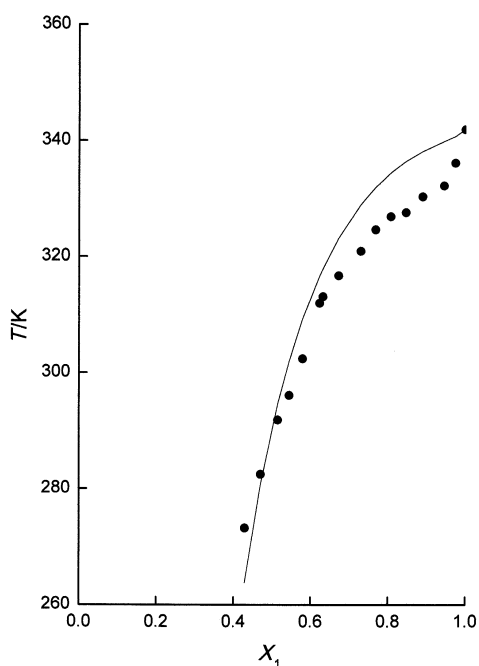


Figure 3. Solubility of $[C_4mim][Cl]$ in H_2O . Points are the experimental results. Solid lines are calculated by means of the NRTL2 equation.

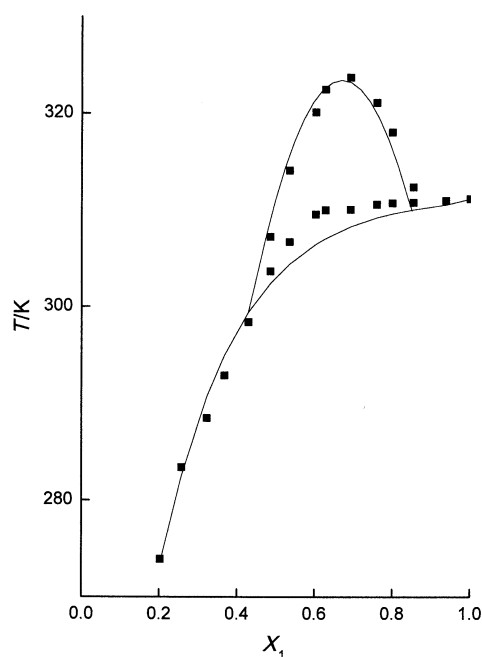


Figure 4. Solid–liquid equilibria and liquid–liquid equilibria of $[C_{10}mim][Cl]$ in H_2O . Points are the experimental results. Solid lines are calculated by the NRTL2 equation without the solid–solid phase transition data.

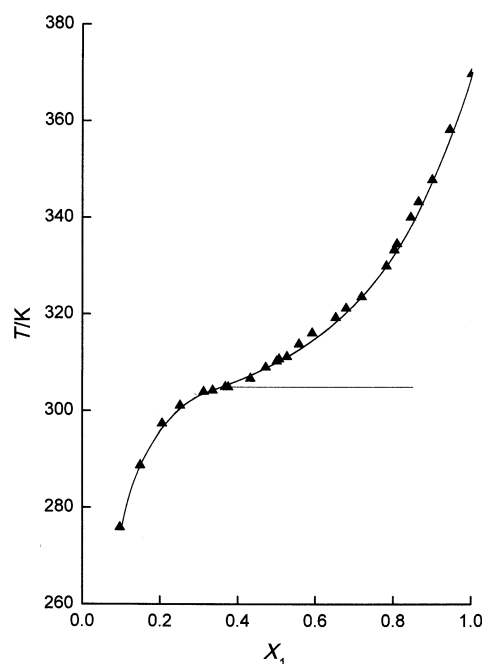


Figure 5. Solubility of $[C_{12}mim][Cl]$ in H_2O . Points are the experimental results. Solid lines are calculated by the NRTL2 equation.

Positive deviations from ideality were found; thus, the solubility is lower than the ideal case; the activity coefficient of the solute is higher than 1 ($\gamma_1 = 1-2$). For $[C_{10}mim][Cl]$, a miscibility gap in water was found (Figure 4 and Table 4). The complete phase diagram of $[C_{12}mim][Cl]$ in alcohols showed a eutectic mixture.^[10]

The solid–solid phase transition for the mixture was not a sharp transition at the same temperature as observed for the

pure salt, but was spread over a range of several degrees in different solvents. This was previously observed for the mixtures of two ionic liquids.^[8b] For the solid solute, the solid–solid phase transition temperature, T_{tr} , is a property of the pure solid and is expected to be not affected by solvent–solute interactions. However, it was noted by us previously^[14] that, for *n*-alkanes, *n*-alkanols, crown-ethers, and cholesterol, changes of phase transition temperatures in different solvents were observed. This has to be connected with the experimental technique and the specific crystalline forms of molecules. It is known that SLE experiments are quite difficult to carry out. The results depend on the procedure (heating or cooling) or for example, on the thermal histories of the materials. When studying transitions these may be triggered by nonhomogeneous nucleation.^[15] In spite of this, substances with long chains or complicated ring structures may present different phases probably with a minimally different enthalpy of solid–solid phase transition than that observed for the pure substance. For example, *n*-alkanes or *n*-alkanols may transform into a rotator phase before melting (usually termed α phase).^[16] This problem was discussed in our earlier work.^[10] There is no doubt that, for our [C₄mim][Cl] and [C₁₂mim][Cl] ionic liquids, some of these features may be expected. For many ILs, one phase with the symmetry of a smectic liquid crystal is observed. It is possible to conclude that solid–solid phase transitions of [C₁₂mim][Cl] may be affected by the presence of the solvent. In other words, it is possible that, in the binary system, transitions are not those encountered in pure ionic liquids, but some of the different rotator phases are involved. X-ray studies are needed in order to clarify this point.

Correlation of SLE: The solubility of solid 1 in a liquid may be expressed in a very general manner by Equation (1):

$$-\ln x_1 = \frac{\Delta H_{m1}}{R} \left(\frac{1}{T_1} - \frac{1}{T_{m1}} \right) + \frac{\Delta H_{tr1}}{R} \left(\frac{1}{T_1} - \frac{1}{T_{tr1}} \right) + \frac{\Delta H_{tr11}}{R} \left(\frac{1}{T_1} - \frac{1}{T_{tr11}} \right) - \frac{\Delta c_{p,m1}}{R} \left(\ln \frac{T_1}{T_{m1}} + \frac{T_{m1}}{T_1} - 1 \right) + \ln \gamma_1 \quad (1)$$

where x_1 is the mole fraction, γ_1 is the activity coefficient, ΔH_{m1} is the enthalpy of fusion, $\Delta c_{p,m1}$ is the difference in solute heat capacity between the solid and liquid at the melting point, T_{m1} is the melting point of the solute (1), and T_1 is the equilibrium temperature. Furthermore, ΔH_{tr1} , ΔH_{tr11} represent the enthalpies of transition and T_{tr1} , T_{tr11} the transition temperatures of the solute (here [C₁₂mim][Cl]). The solubility equation for temperatures below that of the phase transition must include the effect of the transition. Because of the lack of appropriate data representing the difference $\Delta c_{p,m1}$ between heat capacities of the solute in the solid and the liquid states for the systems under investigation, a simplified version of the solubility equation [Eq. (1)] without the $\Delta c_{p,m1}$ term was applied. Equation (1) may be used for the simple eutectic mixtures with full miscibility in the liquid and immiscibility in the solid phases.

In this study three methods are used to derive the solute activity coefficients, γ_1 , from the so-called correlation equa-

tions that describe the Gibbs excess free energy of mixing, (G^E), the UNIQUAC ASM^[17], NRTL1 and NRTL2^[18].

The root-mean-square deviation of temperature [σ_T defined by Eq. (2)] was used as a measure of the goodness of the solubility correlation.

$$\sigma_T = \left(\sum_{i=1}^n \frac{(T_i^{\text{exptl}} - T_i^{\text{calcd}})^2}{n-2} \right)^{1/2} \quad (2)$$

where n is the number of experimental points (including the melting point) and 2 is the number of adjustable parameters. The molar volumes of solutes, V_m (298.15 K), were calculated by the group contribution method^[19] and were assumed to be 186.7, 260.7, 300.6, and 325.8 cm³ mol⁻¹ for $n = 4, 8, 10,$ and $12,$ respectively. The calculations were carried out with the data set of association for 1-octanol and water at 323.15 K, where $K = 12.3$ and the coefficient of heat transfer $-\Delta h_h = 21.73$ kJ mol⁻¹ for alcohol as a solvent^[20] and $K = 1030$ and $-\Delta h_h = 25.60$ kJ mol⁻¹ for water.^[21] In this work, a constant of proportionality similar to the nonrandomness constant of the NRTL1 and NRTL2 equations, the parameter $\alpha_{12} = 0.9$. For every system presented in this work the description of solid–liquid equilibrium was given by the average standard mean deviation $\sigma_T = 1.8$ – 6.8 K, which is an acceptable result. Unfortunately, the solid–solid phase transition of [C₄mim][Cl] was not included in the calculations because of the lack of the DSC data. The results of correlations of imidazole in aliphatic alcohols (C₃–C₁₂) with respect to the occurrence of the alcohols association have presented much better deviations, $\sigma_T = 0.98$ K and $\sigma_T = 1.17$ K for NRTL1 and UNIQUAC ASM, respectively.^[9a] The worst results were obtained for [C₁₂mim][Cl] ($\sigma_T > 7$ K). This is evidence that the high enthalpy of the first ($\alpha_1 \rightarrow \beta_1$) solid–solid phase transition is the main reason for the untypical shape of the liquidus curve and that it influences the possibility of correlation. Possibly, the other models developed for the electrolytes may be used in our next study as fitting equations.

Liquid–liquid equilibria (LLE): The upper critical temperature of the mutual solubility of [C₈mim][Cl] is higher in 1-octanol than in water (Figure 6, Table 5). The coexistence curves are shifted to higher mole fractions of the salt, x_1 . The upper critical solution temperatures and compositions listed in Table 6 increase with increasing number of carbon atoms in the alkyl group on the imidazole ring. It is very difficult to find the whole solid–liquid diagram for the solute mole fraction from zero to one, because the crystallization process of [C₈mim][Cl] is very complicated; the substance presents a weak tendency to crystallize. It can be cooled from the equilibrium liquid state down to low temperatures without crystallizing, entering the metastable supercooled liquid state. For [C₁₀mim][Cl], it was possible to crystallize the salt and to obtain the results of SLE and LLE (Table 4).

1-Octanol/water partitioning: The partition coefficient, P of organic compounds in the 1-octanol/water system is used to assess the bioaccumulation potential and the distribution pattern of drugs and pollutants. The partition coefficient of

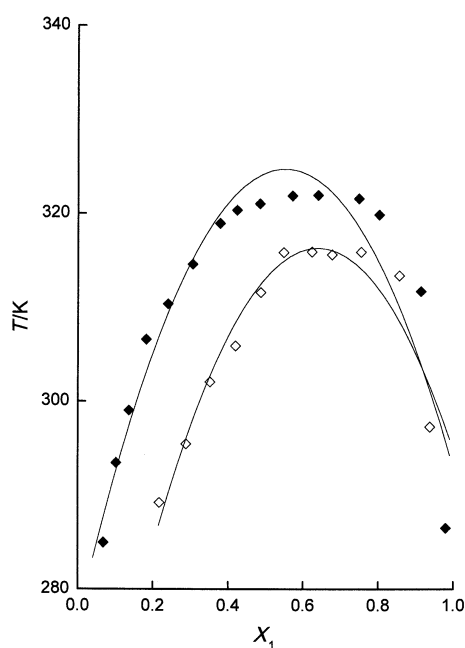


Figure 6. Liquid–liquid equilibria of binary systems: {[C₈mim][Cl] + (◇) 1-octanol, or + (◆) water}. Solid lines are calculated by means of the NRTL2 equation.

Table 5. Liquid–liquid equilibria, LLE of binary mixture {[C₈mim][Cl] + 1-octanol, or water}; x_1' , solute rich and x_1'' , solvent-rich solute mole fraction.

x_1'	$T_{\text{ILLE}}[\text{K}]$	x_1''
1-Octanol		
0.971	289.22	0.217
0.942	295.46	0.288
0.935	302.08	0.351
0.931	305.92	0.419
0.902	311.60	0.486
0.781	315.87	0.548
0.750	315.94	0.623
0.677	315.63	0.748
0.754	315.91	0.621
0.855	313.38	0.515
0.937	297.28	0.300
Water		
0.995	284.96	0.068
0.965	293.47	0.102
0.953	299.04	0.136
0.937	306.60	0.182
0.928	310.36	0.240
0.305	314.62	0.901
0.378	318.96	0.824
0.424	320.36	0.786
0.484	321.04	0.731
0.571	321.88	0.675
0.639	321.95	0.629
0.748	321.59	0.521
0.802	319.87	0.433
0.913	311.72	0.231
0.979	286.50	0.075

imidazoles, which are of great pharmaceutical interest, strongly depends on the hydrogen bond formed by these molecules and is less than one for simple imidazoles on account of the high solubility in water.^[9a] Generally, the

Table 6. Upper critical solution temperature, T^{C} and composition x_1^{f} for {[C_nmim][Cl], where $n = 8, 10 + 1$ -octanol, or water} systems.

System	$T^{\text{C}}[\text{K}]$	x_1^{f}
[C ₈ mim][Cl] + 1-octanol	315.9	0.62
[C ₈ mim][Cl] + water	321.9	0.64
[C ₁₀ mim][Cl] + water	323.7	0.69

hydrophobicity is favorable for bioaccumulation, or the bioconcentration of organic compounds.^[22] Therefore, the low value of the 1-octanol/water partition coefficient is required for new insecticides to avoid bioaccumulation.

Because of the high solubility of ionic liquids in 1-octanol and water, we have used a simple, synthetic, visual method, described below. The experimental results for three temperatures are reported in Table 7. It is evident that the low aqueous solubility of 1-octanol has a negligible influence on

Table 7. Solubilities and experimental data for the partition coefficient at 288.15, 298.15, and 308.15 K.

Substance	x_1^{o}	x_1^{w}	$c_1^{\text{o}*}$ [mol dm ⁻³] ^[a]	$c_1^{\text{w}*}$ [mol dm ⁻³] ^[b]	P	$\log P$
288.15 K						
[C ₄ mim][Cl]	0.3299	0.4969	2.25	4.88	0.46	-0.33
[C ₈ mim][Cl]	0.2112	0.0807	0.99	2.15	0.46	-0.33
[C ₁₀ mim][Cl]	0.2366	0.3185	1.34	2.95	0.45	-0.34
[C ₁₂ mim][Cl]	0.2912	0.1465	1.25	2.32	0.54	-0.27
298.15 K						
[C ₄ mim][Cl]	0.3484	0.5550	2.41	4.97	0.48	-0.31
[C ₈ mim][Cl]	0.3137	0.1307	1.41	2.63	0.54	-0.27
[C ₁₀ mim][Cl]	0.2840	0.4264	1.59	3.08	0.52	-0.29
[C ₁₂ mim][Cl]	0.4595	0.2150	2.15	2.94	0.73	-0.14
308.15 K						
[C ₄ mim][Cl]	0.3976	0.6049	2.66	5.04	0.53	-0.28
[C ₈ mim][Cl]	0.4456	0.2063	1.90	3.03	0.63	-0.20
[C ₁₀ mim][Cl]	0.5155	0.5689	2.26	3.18	0.71	-0.15
[C ₁₂ mim][Cl]	0.5507	0.4559	2.12	2.88	0.74	-0.13

[a] Calculated with the density of 1-octanol equal to 0.82260 (288.14 K), 0.82260 (298.15 K), and 0.81515 (308.15 K). [b] Calculated with the density of water equal to 1.0010 (288.15 K), 0.99741 (298.15 K), and 0.99382 (308.15 K). The density of subcooled solutes at 298.15 K (molar volumes mentioned in the text) were assumed to be constant at three temperatures.

the aqueous solubility of [C_nmim][Cl]. On the other hand, the rather large amount of water present in the 1-octanol phase (“solute-free” $x_{\text{w}}^{\text{o}} = 0.29$),^[23] changes considerably the [C_nmim][Cl] solubility in the 1-octanol phase even if a simple linear dependence of solubility for binary “solute free” solvent was assumed. Corresponding values of the [C_nmim][Cl] solubilities in mutually saturated solvent as a molar concentration in water-saturated 1-octanol, ($c_1^{\text{o}*}$) and 1-octanol-saturated water, ($c_1^{\text{w}*}$) are given in Table 7. The solute partition coefficient, defined as $P = c_1^{\text{o}*}/c_1^{\text{w}*}$, of [C_nmim][Cl] was shown to be less than one. Indeed, the 1-octanol/water partition coefficient for ILs used as a solvents in new “green technology”, is used to evaluate the hydrophobicity of a solvent in environmental science. The influence of temperature (Figure 7) is not higher than 9% per 10K.

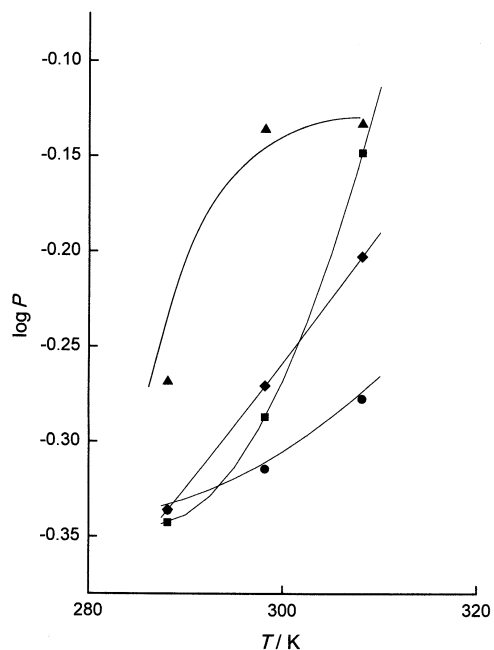


Figure 7. $\log P$ as a function of the temperature for (●) $[\text{C}_4\text{mim}][\text{Cl}]$; (◆) $[\text{C}_8\text{mim}][\text{Cl}]$; (■) $[\text{C}_{10}\text{mim}][\text{Cl}]$; (▲) $[\text{C}_{12}\text{mim}][\text{Cl}]$. Solid lines are calculated by means of polynomials.

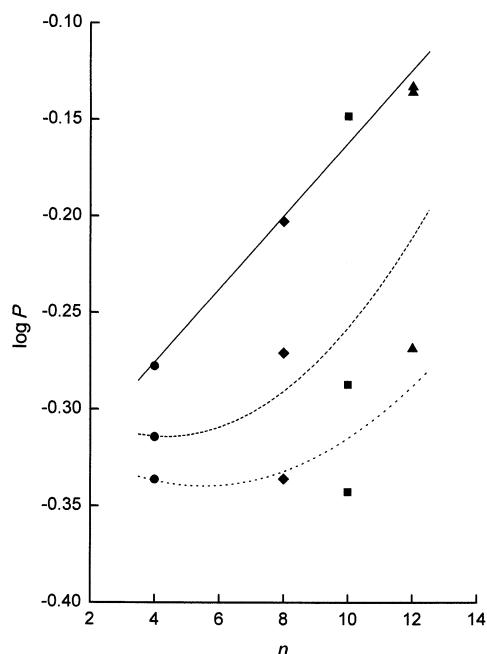


Figure 8. $\log P$ as a function of n , the number of carbon atoms in the chain of the alkyl group in the salt: (●) $n=4$; (◆) $n=8$; (■) $n=10$; (▲) $n=12$ at $T=288.15\text{ K}$ (••••); $T=298.15\text{ K}$ (---), and $T=308.15\text{ K}$ (—).

The function of $\log P$ versus the number of carbon atoms in the chain of the alkyl group n in the ionic liquid is shown in Figure 8. As n of the alkyl group increases the value of the octanol/water partition coefficient increases (is less negative). The results show that rather short chain substituents may be suggested for “green solvents” for new technologies.

Conclusions

The phenomenon of four solid–solid phase transitions for $[\text{C}_{12}\text{mim}][\text{Cl}]$ and one for the $[\text{C}_4\text{mim}][\text{Cl}]$ ionic liquids have been observed in the temperature range from 200 to 400 K. The solubility of $[\text{C}_n\text{mim}][\text{Cl}]$ in 1-octanol and water depends on the number of carbon atoms in the chain of the alkyl group in the ionic liquid. Results of partition coefficients reported in this paper indicate that ILs based on a simple imidazole ring show a weak affinity toward bioaccumulation; this has been previously observed for simple imidazole molecules.^[9a]

Experimental Section

Materials: The $[\text{C}_n\text{mim}][\text{Cl}]$ compounds produced by Solvent Innovation GmbH, Cologne (Germany) were used as-purchased without further purification. The purity was ≥ 98 mass-% for every substance. 1-Octanol from Sigma-Aldrich Chemie GmbH, Steinheim (Germany) was fractionally distilled to >99.8 mass-% purity. Solvent was stored over freshly activated molecular sieves of type 4 Å (Union Carbide). Doubly distilled and degassed water was used for the solubility measurements.

Procedures: Differential scanning microcalorimetry (DSC) was used to determine the melting point ($T_{\text{m}i}$), the enthalpies of fusion ($\Delta H_{\text{m}i}$), temperatures of solid–solid phase transition I ($\alpha_1 \rightarrow \beta_1$), II ($\beta_1 \rightarrow \gamma_1$), III and IV ($T_{\text{tr-IV}}$), and enthalpies of solid–solid phase transitions ($\Delta H_{\text{tr-IV}}$) as well as the glass transition in different sequence for different salts. Molar enthalpies of fusion and solid–solid phase transitions have been measured with the differential scanning microcalorimeter Perkin–Elmer Pyris 1. Measurements of the fusion enthalpies were carried out at a scan rate of 2 or 10 K min^{-1} with a power sensitivity of 16 mJ s^{-1} . The instrument was calibrated against an indium sample with 99.9999 mol-% purity. The calorimetric accuracy was $\pm 1\%$ and the calorimetric precision was $\pm 0.5\%$. Solid solubilities were determined by means of a dynamic (synthetic) method, described in detail previously.^[24] Mixtures of solute and solvent were prepared by weighing the pure components to within 1×10^{-4} g. The sample of solute and alcohol or water were heated very slowly ($< 2\text{ K h}^{-1}$ near the equilibrium temperature) with continuous stirring inside a Pyrex glass cell placed in a thermostat. The crystal disappearance temperatures, detected visually, were measured with a calibrated Gallenkamp Auto-therm II thermometer totally immersed in the thermostating liquid. Measurements were carried out over a wide range of solute mole fraction from 0.1 to 1.0. The thermometer was calibrated on the basis of the ITS-90 temperature scale. The accuracy of temperature measurements was $\pm 0.01\text{ K}$ while the error of mole fraction did not exceed $\delta x_1 = 0.0005$. The difference compared to our previous published results of solubilities^[9, 10] (and the references therein) is that every experimental point was obtained from a new sample. Additionally, it was found that the solution-crystallization procedure was quite slow and difficult, thus the solubility measurements were very time-consuming.

- [1] a) J. D. Holbrey, K. R. Seddon, *Clean Prod. Process.* **1999**, *1*, 223–236; b) L. C. Branco, J. N. Rosa, J. J. Moura Ramos, C. A. M. Alfonso, *Chem. Eur. J.* **2002**, *8*, 3671–3677.
- [2] a) K. R. Seddon, *J. Chem. Technol. Biotechnol.* **1997**, *68*, 351–356; b) K. R. Seddon, *Molten Salts Forum* **1998**, p. 53–62; c) T. Welton, *Chem. Rev.* **1999**, *99*, 2071–2084.
- [3] a) Y. Chauvin, H. Olivier-Bourbigou, *Chemtech* **1995**, *25*, 26–30; b) Y. Chauvin, *Actual. Chimique* **1996**, 44–46; c) M. Freemantle, *Chem. Eng. News* **1998a**, *76*, 32–37; d) M. Freemantle, *Chem. Eng. News* **1998b**, *76*, 12; e) M. Freemantle, *Chem. Eng. News* **1999**, *77*, 23–24; f) C. L. Hussey, *Adv. Molten Salt Chem.* **1983**, *5*, 185–230; g) C. L. Hussey, *Pure Appl. Chem.* **1988**, *60*, 1763–1772; h) K. R. Seddon, *Kinet. Catal.* **1996**, *37*, 693–697.
- [4] a) M. J. Earle, K. R. Seddon, *Pure Appl. Chem.* **2000**, *72*, 1391–1394; b) P. Wasserscheid, W. Keim, *Angew. Chem.* **2000**, *112*, 3926–3945;

- Angew. Chem. Int. Ed.* **2000**, *39*, 3772–3789; c) D. W. Rooney, K. R. Seddon, in *Handbook of Solvents* (Ed.: G. Wypych), ChemTech, **2000**, p. 1495.
- [5] C. L. Hussey, *Pure Appl. Chem.* **1988**, *60*, 1763–1772.
- [6] J. L. Anthony, E. J. Maginn, J. F. Brennecke, *J. Phys. Chem. B* **2001**, *105*, 10942–10949.
- [7] a) K. R. Seddon, A. Stark, M. Torres, *J. Pure Appl. Chem.* **2000**, *72*, 2275–2287; b) S. N. Aki, J. F. Brennecke, A. Samanta, *Chem. Commun.* **2001**, 413–414; c) L. A. Blanchard, J. F. Brennecke, *Ind. Eng. Chem. Res.* **2001**, *40*, 287–292; d) G. Law, P. R. Watson, *Chem. Phys. Lett.* **2001**, *345*, 1–4; e) A. J. Carmichael, K. R. Seddon, *J. Phys. Org. Chem.* **2000**, *13*, 591–595.
- [8] a) J. D. Holbrey, K. J. Seddon, *J. Chem. Soc. Dalton Trans.* **1999**, 2133–2139; b) C. M. Gordon, J. D. Holbrey, A. R. Kennedy, K. R. Seddon, *J. Mater. Chem.* **1998**, *8*, 2627–2636; c) W. Xu, D. Zhang, C. Yang, X. Jin, Y. Li, D. Zhu, *Synth. Met.* **2001**, *122*, 409–412; d) K. A. Abdul-Sada, M. P. Atkins, B. Ellis, P. K. G. Hodgson, M. L. M. Morgan, K. R. Seddon, *World Pat.* **1995**, WO9521806; e) K. A. Abdul-Sada, P. W. Ambler, P. K. G. Hodgson, K. R. Seddon, N. J. Stewart, *World Pat.* **1995**, WO9521871; f) C. J. Bowlas, D. W. Bruce, K. R. Seddon, *Chem. Commun.* **1996**, 1625–1626; g) K. M. Lee, C. K. Lee, I. J. B. Lin, *Chem. Commun.* **1997**, 899–900; h) J. G. Huddleston, H. D. Willaner, R. P. Swotloski, A. E. Visser, R. D. Rogers, *Chem. Commun.* **1998**, 1765–1766.
- [9] a) U. Domańska, M. K. Kozłowska, M. Rogalski, *J. Chem. Eng. Data* **2002**, *1*, 8–16; b) U. Domańska, M. K. Kozłowska, M. Rogalski, *J. Chem. Eng. Data* **2002**, *47*, 456–466; c) U. Domańska, E. Bogel-Lukasik, *J. Chem. Eng. Data* **2003**, in press; d) M. Rogalski, U. Domańska, D. Czyrny, D. Dyczko, *Chem. Phys.* **2002**, *285*, 355–370.
- [10] U. Domańska, E. Bogel-Lukasik, R. Bogel-Lukasik, *J. Phys. Chem. B* **2003**, *107*, 1858–1863.
- [11] a) A. Müller, *Proc. R. Soc. London Ser. A* **1932**, *138*, 514–517; b) M. Dirand, M. Boroukba, V. Chevalier, D. Petitjean, D. E. Behar, V. J. Ruffier-Meray, *Chem. Ing. Data* **2002**, *47*, 115–135; c) I. D. Hoffman, B. F. Decker, *J. Phys. Chem.* **1932**, *138*, 514–521; d) A. Craievich, J. Doucet, J. Denicolo, *Phys. Rev. B* **1985**, *32*, 4164–4168.
- [12] a) A. Elaiwi, P. B. Hitchcock, K. R. Seddon, N. Srinivasan, Y. M. Tan, T. Welton, J. A. Zora, *J. Chem. Soc. Dalton Trans.* **1995**, 3467–3472; b) J. Dupont, P. A. Z. Suarez, R. F. de Souza, R. A. Burrow, J. P. Kintzinger, *Chem. Eur. J.* **2000**, *6*, 2377–2379.
- [13] M. Kosmulski, B. Tendaj, *Przemysł Chemiczny* **2001**, *8017*, 280–285.
- [14] a) U. Domańska, K. Domański, *Fluid Phase Equilib.* **1991**, *68*, 103–114; b) U. Domańska, *Fluid Phase Equilib.* **1996**, *114*, 175–188; c) J. A. Gonzalez, M. Szurgocińska, U. Domańska, *Fluid Phase Equilib.* **2002**, *200*, 349–374; d) U. Domańska, *Polish. J. Chem.* **1998**, *72*, 925–939; e) U. Domańska, C. Klofutar, Ś. Paljk, *Fluid Phase Equilib.* **1994**, *97*, 191–200.
- [15] J. C. Miltenburg, L. Oonk, J. Ventola, *J. Chem. Eng. Data* **2001**, *46*, 90.
- [16] a) T. Yamamoto, K. Nozaki, T. Hara, *J. Chem. Phys.* **1990**, *92*, 631–638; b) A. Watanabe, *Bull. Chem. Soc. Jpn.* **1961**, *34*, 1728–1734; c) J. D. Hoffman, C. P. Smyth, *J. Am. Chem. Soc.* **1949**, *71*, 431–439; d) E. B. Sirota, H. E. King, D. H. Singer, H. H. Shao, *J. Chem. Phys.* **1993**, *98*, 5809–5815; e) E. B. Sirota, H. E. King, G. J. Hugues, W. K. Wan, *Phys. Rev. Lett.* **1992**, *68*, 492–496.
- [17] I. Nagata, *Fluid Phase Equilib.* **1985**, *19*, 153–174.
- [18] I. Nagata, Y. Nakamiya, K. Katoh, J. Kayabu, *Thermochim. Acta* **1981**, *45*, 153–165.
- [19] A. F. M. Barton, *CRC Handbook of Solubility Parameters*, CRC Press, Boca Raton, FL, **1985**, p. 64.
- [20] T. Hofman, I. Nagata, *Fluid Phase Equilib.* **1986**, *28*, 233–252.
- [21] A. Nath, E. Bender, *Fluid Phase Equilib.* **1981**, *7*, 289–293.
- [22] S. I. Sandler, H. Orbey, *Fluid Phase Equilib.* **1993**, *82*, 63–69.
- [23] A. J. Dallas, P. W. Carr, *J. Chem. Soc. Perkin Trans. 2* **1992**, 2155–2160.
- [24] U. Domańska, *Fluid Phase Equilib.* **1986**, *26*, 201–220.

Received: October 21, 2002 [F4516]